

PROIECTAREA LONJERONULUI MG (MG'S WING SPAR DESIGN)

CHELEMEN Dennis Ștefan

Facultatea: Inginerie Aerospațială, Specializarea: Construcții aerospațiale, Anul de studii: II,
e-mail: dennis.chelemen@stud.aero.upb.ro

Conducători științifici: Prof. dr. ing. **Cristian PETRE**, Conf. dr. ing. **Florin BACIU**

ABSTRACT: In this paper we aim to create a new and improved spar design adapted to an aircraft that is currently in development. One might ask what is the optimal design for such a task, and might think that there are just a few options to choose from. While there are many possibilities and variations to add to a structural design of an aircraft, they might not be perfectly efficient for every design, thus we created a spar design fitted for our task, which combined 2 of the most already used concepts in this field, that in the end turned out to be more efficient than the classical ones.

1. Introduction

In this paper we analyze new methods to design an aircraft's wing spar (that is currently in development; MG-017). The present project suggests a new type of spar beam, which is shown to be more reliable for economic and structural reasons, being more efficient than those already used by similar aircraft.

The airplane, MG-017 is an Unmanned Air Vehicle (UAV) whose purpose is to transport medical equipment such as blood bags

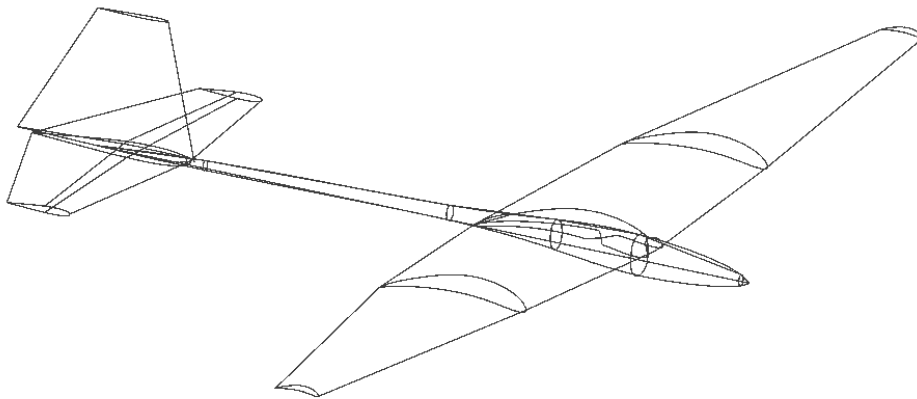


Fig.1 (Representation of the aircraft in the XFLR5 software)

1.2 Aircraft details.

Wing is composed of 3 sections (one central and two adjacent) totaling 1.826m in span, using a dihedral and torsion angle. At the moment it is estimated that the aircraft is going to weight ~3.9kg.

1.3 exposing the problem.

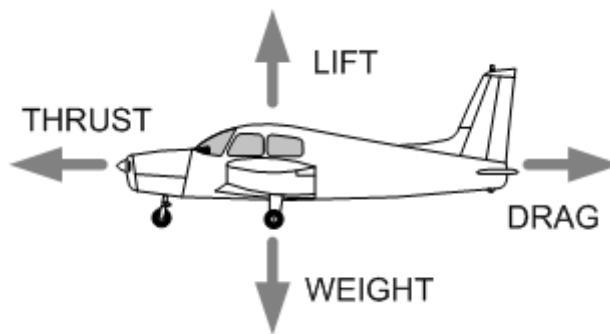


Fig. 2 (The forces acting on the aircraft¹)(<http://www.langleyflyingschool.com/>)

In various applications, the lifting force of the aircraft is considered to act at a single point (Center of pressure) as well as the forward resistance force. But this is not true, as they are more of a force distributed unevenly along the body that meets the air.

In order to generate more lift and have a more efficient flight, the planes change their angle of attack (the angle between the flight direction and the wind direction), which leads to a higher wing load. So for the study of this aircraft we consider an angle of attack of 7° and that it flies at a speed of 9 m / s. We consider relevant only the lift and drag force, summarizing the phenomenon to a problem of compound stresses. Moreover, considering the whole wing as a bar, which is embedded in the area where the fuselage is attached.

1.4 Solving the Problem

The first step in solving the problem is to determine the intensity of the forces acting on the wing, which has been reduced to a bar. For this it is necessary to apply some notions of advanced aerodynamics, such as the Schrenck² method from which the local lift force results:

$$p(y) = \rho U_\infty \Gamma(y) \quad [\text{N/m}] \quad (1)$$

$$= \frac{\rho}{2} U_\infty^2 \cdot c C_z(y)$$

$$= \frac{\rho}{2} U_{\infty}^2 \cdot c(y) C_l(y)$$

ρ - air density; U - air speed from infinity, $c(y)$ - chord line in that point, $C_l(y)$ lift coefficient

Similarly, we obtain the local drag force.

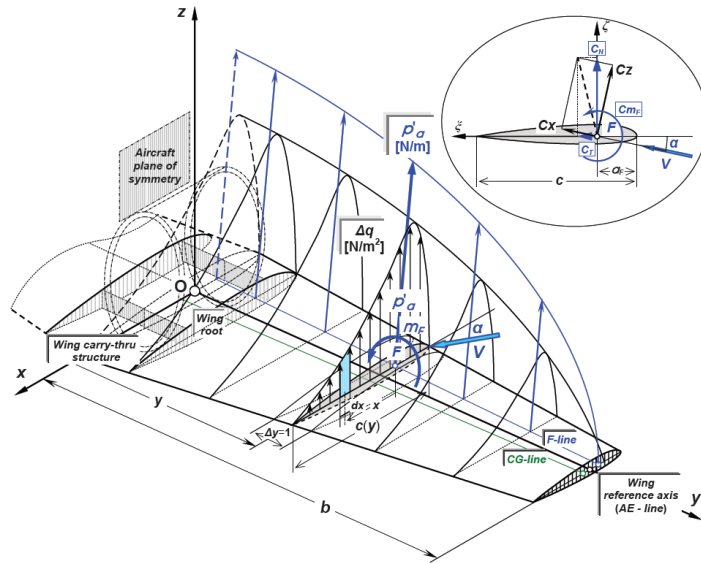


Fig.3 Lift distribution on a wing³

Applying the formula mentioned above for as many points on the semi-wing as possible (the problem is symmetrical, so for simplicity we will work only on one side), we obtain the following lift distribution:

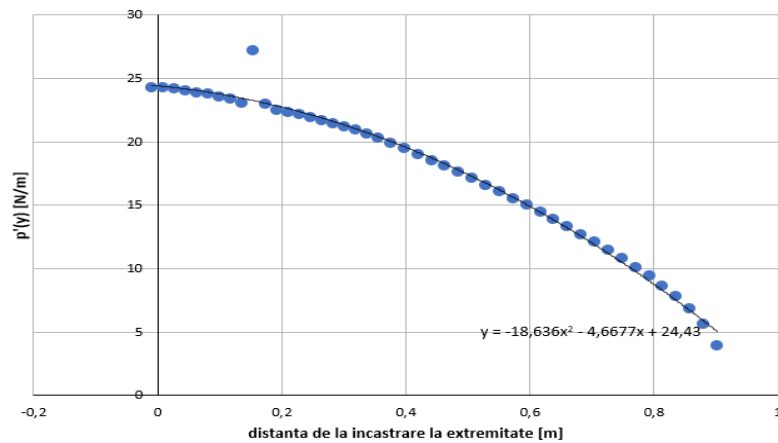


Fig.4 Load distribution on the MG-017 semi-wing

There are points that deviate significantly from the approximation curve, but they occur as a result of extrapolation problems from the polar graphs of the XFRLR5 program profile that determined the values $c(y)$ and $C(y)$, on the graph we can also see the function of the distribution. In the case of forward resistance force distribution, there were many more points that deviated from the curve path, and they had to be changed manually.

We know that the intensity of the force acting on a bar is equal to the area under the curve joining the points of maximum force of the points on the bar that replaces the wing, in our case, to determine the force acting on the wing, we must apply the following relation:

$$T_P(y) = - \int_y^b f(t) dt \text{ [N]} \quad (2)$$

And to determine the moment, we aim to integrate the shear force as follows:

$$M_P(y) = - \int_y^b T_P(t) dt \text{ [Nm]} \quad (3)$$

To get the shear force and moment diagrams, we can put them on a graph as shown here:

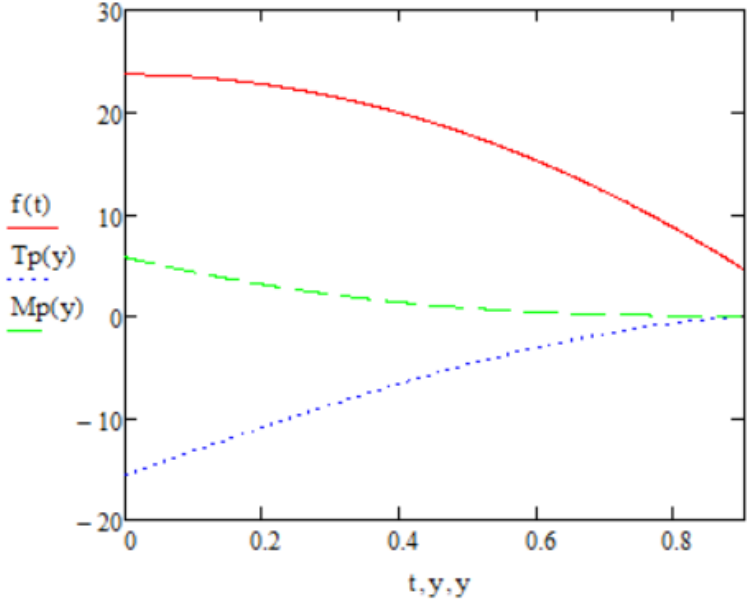


Fig. 5 Shear force and moment diagrams in the case of lift force.

Similarly, the algorithm is executed for the forward resistance force:

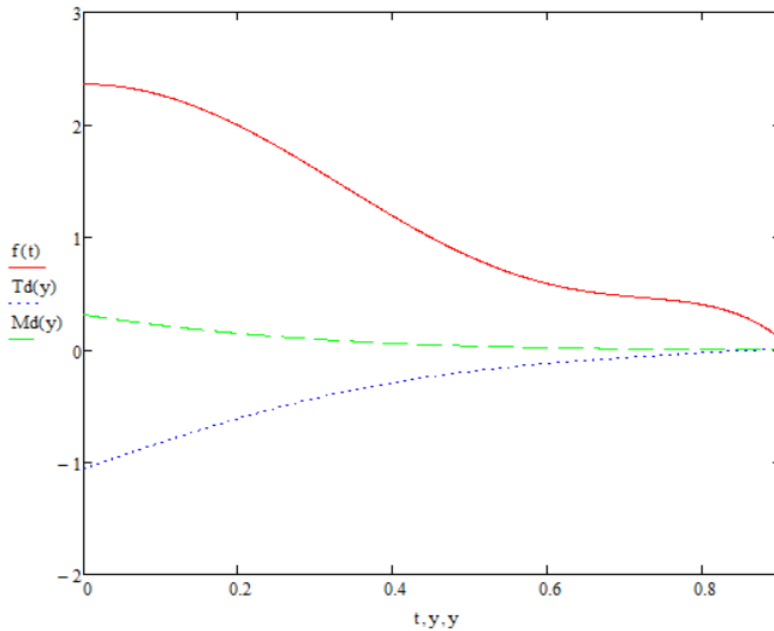


Fig. 6 Shear force and moment diagrams in the case of drag force.

With this data, we can do the pre-sizing calculation of the spar. It is noticed that the critical section is in the embedded region.

1.5 Spar choosing

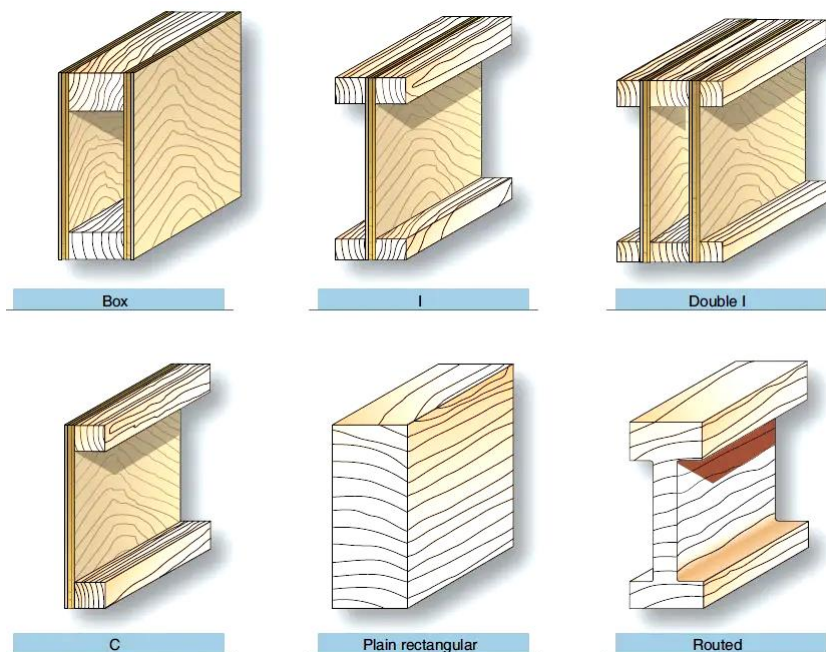


Fig. 7 Models of wing spar designs already used⁴. (<https://www.aircraftsystemstech.com/2019/05/repair-of-wood-aircraft-components.html>)

The innovation that this work brings is the combination of 2 existing spar beam designs. The 'I' and 'Routed' shapes are ideal if we have shear force only vertically, but, as we know from

Chapter 1.3, we also have the forward resistance force, where the ‘C’ shape is the most ideal. Therefore, we wanted to investigate what would happen to the dimensions of the spar if we were to design two ‘I’ shaped beams, one of which would be smaller and arranged at 90°, as in fig. 8.

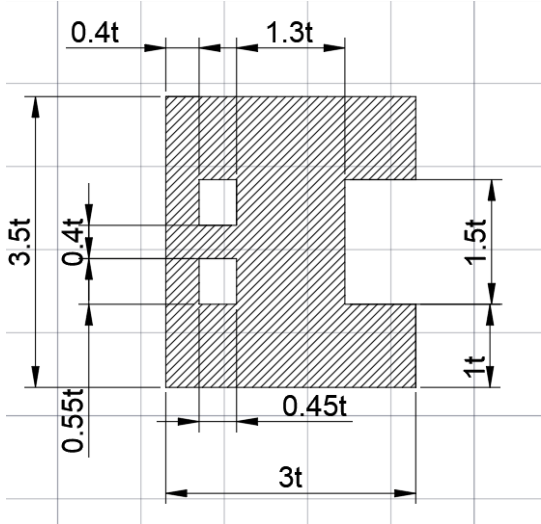


Fig. 8 section for ‘2IC’ beam

The above piece derives, as mentioned above, from a type ‘I’ shape which we will analyze for comparison, taking the same proportions:

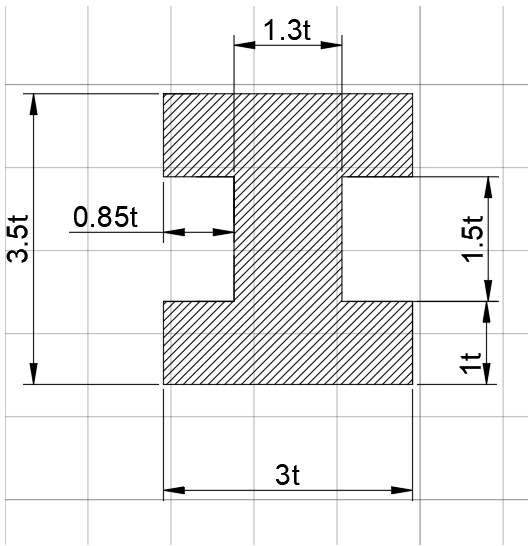


Fig. 9 section for ‘I’ beam.

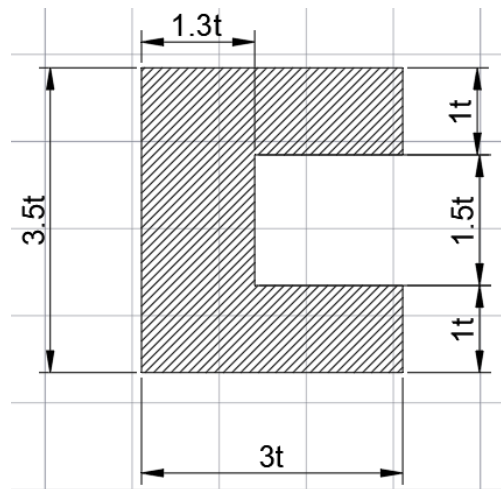


Fig. 10 section for 'C' beam.

Based on the data provided by the diagrams and the figures above, we can calculate the stresses in the beams (embedded) with the relation:

$$\sigma = \frac{M_{ech}}{w_y} = \frac{\sqrt{M_P^2 + M_d^2}}{w_y} \text{ [MPa]} \quad (4)$$

Result that must be less than the maximum allowable tension, which we will consider 70MPa (Balsa, aviation board)

Following the calculations, for the spar '2IC' a $t_{min} = 2.001$ mm is obtained, and for the one in the 'I' shape, a $t_{min} = 2.41$ mm. But these numbers for safety are multiplied by a factor of ,2.5'. So for '2IC', the t becomes 5.0025 mm and for 'I', the t equals 6.025 mm. Performing some volume calculations, it turns out that the '2IC' spar needs 221576.46 mm³ of material, and the 'I' shaped one needs more, 260308mm³. Performing the calculations analogous to the type 'C', we get that we need 202415 mm³ of material, but the final calculation must also calculate the fact that in flight there are aerodynamic moments, gusts of wind, phenomena that twist the wing, a process in which the shape ,2IC' may hold up better.

2. Current Stage

Currently only the pre-sizing calculations of the spar are completed. In the coming weeks, numerical simulations will be made, analyzing the 3 spars in more detail (the aerodynamic moment will be taken into account, possible twists, etc.), and then one will be chosen, which will lead to the development of the aircraft structure.

3. Conclusions

As shown in Chapter 1.5, the '2IC' shape of the beam, is more efficient because it requires less material, therefore a lower cost and a lower weight. In the following analyzes of this spar, we propose that the '2IC' form be subjected to twists, thus taking into account one more moment, the aerodynamic moment generated by the wing.

4. Bibliography

- [1]. Unknown author – Langley Flying school.
- [2]. Unknown author (2011), "Proiect aripa", 23.
- [3]. Unknown author (2017), "Forces on wings", 16.
- [4]. Unknown author " 'Repair of Wood Aircraft Components' in: 'Repair of Wood Aircraft Structures - Part 3'